RSC Advances

PAPER

View Article Online
View Journal | View Issue

Cite this: *RSC Adv.*, 2016, **6**, 76736

Synthesis of C_2 oxygenates from syngas over Rh–Mn–Li/SiO_2 catalysts: effect of supports prepared using different ammonia concentrations

Jun Yu,[a] Dongsen Mao,*[a] Dan Ding[a] and Guanzhong Lu*[ab]

Received 27th June 2016
Accepted 9th August 2016

DOI: 10.1039/c6ra16404h

www.rsc.org/advances

The effects of surface properties of the monodispersed SiO_2 prepared using different ammonia concentrations on the catalytic performance of Rh–Mn–Li/SiO_2 for CO hydrogenation to C_2 oxygenates were investigated. The investigation based on the catalytic performance and characterizations of the catalysts suggested that the catalytic performance was relatively stable on the Rh–Mn–Li catalyst supported on the SiO_2 prepared using high ammonia concentration, which is attributed to the steady state of the metals supported on it. However, the rough surface of SiO_2 prepared using a low ammonia concentration resulted in easy agglomeration of the metals. Correspondingly, the size of Rh particles increased and the isolated Rh^+ sites decreased in the reaction process, leading to the decrease of C_2 oxygenate selectivity of the catalyst as a function of time.

1. Introduction

One of the largest social challenges today is the quest for alternative fuels, which would reduce greenhouse gas emissions as well as the heavy dependence on depleting fossil fuels.[1] The synthesis of C_2 oxygenates (*e.g.*, ethanol, acetaldehyde and acetic acid) from syngas, which can be produced from non-petroleum carbon resources including natural gas, coal, and biomass, constitutes an alternative pathway for the production of clean fuels and chemicals.[2–5] So far, Rh-based/SiO_2 catalysts have been shown to be active for C_2 oxygenate synthesis from syngas,[6–8] however, the CO conversion and selectivity of C_2 oxygenates are still not enough for practical use. In order to further improve the catalytic properties of Rh-based/SiO_2 catalysts, the modification of additives and SiO_2 supports has been investigated continuously in the past decades.[9–17]

In our previous studies, it has been found that the catalytic performance of the Rh–Mn–Li/SiO_2 catalyst for the synthesis of C_2 oxygenates from CO hydrogenation was enhanced greatly when a commercial SiO_2 was replaced by a monodispersed SiO_2 prepared by the Stöber method.[18,19] The excellent performance of this catalyst can be mainly attributed to the special surface properties of the monodispersed SiO_2. It is widely accepted that the properties of supports have a considerable influence on the Rh-based catalysts, which finally leads to disparities in the catalytic performance. Solymosi *et al.*[11] proposed that surface hydroxyl groups on silica play an important role in the change in the oxidation state of the metal, and the active sites of Rh^+ can be formed *via* an oxidation of the Rh^0 clusters by the surface OH groups of SiO_2. Chen *et al.*[20] observed that the Rh particles were more homogeneously dispersed when 14–20 mesh silica was used instead of 20–40 mesh as a support for Rh–Mn–Li catalyst. As a result, the space time yield and selectivity of C_2^+ oxygenates were significantly increased from 338.6 g (kg^{-1} h^{-1}) and 49.2% to 618.4 g (kg^{-1} h^{-1}) and 54.6%, respectively ($T = 300$ °C, $P = 3$ MPa, SV = 12 500 h^{-1}). Bao and co-workers found that the different electronic properties of inside and outer carbon nanotubes surface can change the Rh–Mn interaction, which resulted in the different CO adsorption behavior and catalytic performance.[21]

In fact, the morphology and surface properties of SiO_2 prepared by the Stöber method can be modified by the ammonia concentration, which may influence on the supported metal components. Thus, the effects of surface properties of the monodispersed SiO_2 prepared by different ammonia concentration on the catalytic performance of Rh–Mn–Li/SiO_2 catalysts were investigated in this work. Then, CO hydrogenation performance of the catalysts was correlated with the interaction extents among Rh, Mn and SiO_2.

2. Experimental section

2.1. Catalyst preparation

The monodispersed SiO_2 was prepared by the Stöber method.[22] In a typical synthesis, the mixture solution of 21 ml tetraethylorthosilicate (TEOS, 99.5%, SCRC) and 50 ml anhydrous ethanol (99.7%, SCRC) was added slowly into the mixed

[a]*Research Institute of Applied Catalysis, School of Chemical and Environmental Engineering, Shanghai Institute of Technology, Shanghai 201418, P. R. China. E-mail: dsmao@sit.edu.cn; gzhlu@ecust.edu.cn; Fax: +86-21-60873625; +86-21-64253824*

[b]*Key Laboratory for Advanced Materials and Research Institute of Industrial Catalysis, East China University of Science and Technology, Shanghai 200237, P. R. China*

solution of 76 ml ammonia (26 vol%, SCRC) and 200 ml anhydrous ethanol. Then, this synthesis solution was aged for 4 h and separated centrifugally at 7000 r.p.m. Finally, the collected product was washed with de-ionized water and dried at 70 °C for 12 h, which was denoted as SiO_2(H). The SiO_2(L) was synthesized by the same steps as above, but the amount of ammonia was changed by 21 ml. Before being used, the SiO_2 was calcined in static air at 350 °C for 4 h.

$RhCl_3$ hydrate (Rh ~36 wt%, Fluka), $Mn(NO_3)_2 \cdot 6H_2O$ (99.99%, SCRC), Li_2CO_3 (99.5%, SCRC), and SiO_2 mentioned above were used in catalyst preparations. Catalysts were prepared by co-impregnation to incipient wetness of the prepared SiO_2 (1.0 g) with an aqueous solution of $RhCl_3$ hydrate and precursors of the promoters (Mn and Li), followed by drying at 90 °C for 4 h, and then at 120 °C overnight before being calcined in air at 350 °C for 4 h. For both of the catalysts, Rh loading was 1.5 wt% and the weight ratio of Rh : Mn : Li = 1.5 : 1.5 : 0.07. The obtained catalysts were denoted as RML/SiO_2(H) and RML/SiO_2(L). In addition, the used catalysts were denoted as RML/SiO_2(H)-UD and RML/SiO_2(L)-UD.

2.2. Testing of the catalytic activity

CO hydrogenation was performed in a fixed-bed micro-reactor with length ~350 mm and internal diameter ~5 mm. The catalyst (0.3 g) diluted with inert α-alumina (1.2 g) was loaded between quartz wool and axially centered in the reactor tube, with the temperature monitored by a thermocouple close to the catalyst bed. Prior to reaction, the catalyst was heated to 400 °C (heating rate ~ 3 °C min^{-1}) and reduced with H_2/N_2 (10% v/v, total flow rate = 50 ml min^{-1}) for 2 h at atmospheric pressure. The catalyst was then cooled down to 300 °C and the reaction started as gas flow was switched to a H_2/CO mixture (molar ratio of H_2/CO = 2, total flow rate = 50 ml min^{-1}) at 3 MPa. All post-reactor lines and valves were heated to 150 °C to prevent product condensation. The products were analyzed online (Agilent GC 6820) using a HP-PLOT/Q column (30 m, 0.32 mm ID) with detection with an FID (flame ionization detector) and a TDX-01 column with a TCD (thermal conductivity detector). The conversion of CO was calculated based on the fraction of CO that formed carbon-containing products according to: % conversion = $(\sum n_i M_i / M_{CO}) \times 100\%$, where n_i is the number of carbon atoms in product i; M_i is the percentage of product i detected, and M_{CO} is the percentage of CO in the feed. The selectivity of a certain product was calculated based on carbon efficiency using the formula $n_i C_i / \sum n_i C_i$, where n_i and C_i are the carbon number and molar concentration of the ith product, respectively.

2.3. Catalyst characterization

The X-ray powder diffraction (XRD) spectra of samples were obtained on a Rigaku D/MAX-IIIA X-ray diffractometer with CuKα (λ = 0.15418 nm). The specific surface area (S_{BET}), pore volume (V_p), and pore diameter (D_p) of samples were obtained by N_2 adsorption at −196 °C on a Micromeritics ASAP 2020 apparatus. Transmission electron microscopy (TEM) images were obtained by JEM-2100 operated at 200 kV.

H_2 temperature-programmed reduction (H_2-TPR) was carried out in a quartz micro-reactor. 0.1 g of the sample was first pretreated at 350 °C in O_2/N_2 (20% v/v) for 1 h prior to a TPR measurement. During the TPR experiment, H_2/N_2 (10% v/v) was used at 50 ml min^{-1} and the temperature was ramped from room temperature (RT) to 650 °C at 10 °C min^{-1} while the effluent gas was analyzed with a TCD detector.

CO adsorption was studied using a Nicolet 6700 FTIR spectrometer equipped with a DRIFT (diffuse reflectance infrared Fourier transform) cell with CaF_2 windows. The sample in the cell was pretreated in H_2/N_2 (10% v/v) at 400 °C for 2 h, and then the temperature was dropped to RT. After the cell was outgassed in vacuum to $<10^{-3}$ Pa, the background was scanned. After introducing CO into the IR cell ($p_{CO} = 8.0 \times 10^3$ Pa), the IR spectrum of CO adsorbed on the catalyst was recorded. The concentration of CO was higher than 99.97%, and it was pretreated by dehydration and deoxygenization before being used. The spectral resolution was 4 cm^{-1} and the scan times were 64.

The temperature-programmed surface reaction (TPSR) experiment was carried out as follows: after the catalyst was reduced at 400 °C in H_2/N_2 (10% v/v) for 2 h, it was cooled down to RT and CO was introduced for adsorption for 0.5 h; afterward, the H_2/N_2 was swept again, and the temperature was increased at the rate of 10 °C min^{-1} with the QMS as the detector to monitor the signal of CH_4 (m/z = 15).

3. Results and discussion

3.1. Catalytic activities

Fig. 1 and Table 1 show the catalytic performances of the two catalysts for CO hydrogenation. It can be seen that the catalytic performance of RML/SiO_2(L) and RML/SiO_2(H) exhibited

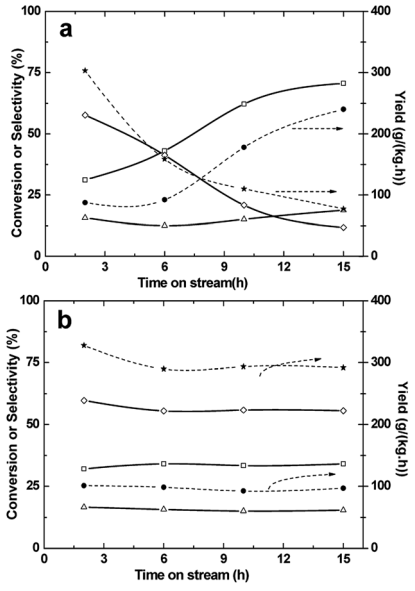

Fig. 1 The catalytic performance *vs.* time-on-stream for the catalysts of (a) RML/SiO_2(L) and (b) RML/SiO_2(H): CO conversion (Δ), selectivity of C_2 oxygenates (◇), selectivity of hydrocarbon (□), STY of C_2 Oxy (★), STY of hydrocarbons (●).

Table 1 CO hydrogenation performance on the catalysts after reaction for 2 h[a]

Catalyst	CO conv. (C%)	Selectivity of products[b] (C%)							STY (C_2 Oxy) (g (kg^{-1} h)$^{-1}$)	STY (HC) (g (kg^{-1} h^{-1}))
		CO_2	MeOH	AcH	EtOH	C_2 Oxy[c]	HC[d]	Other Oxy[e]		
RML/SiO_2(L)	15.7	6.7	1.7	35.2	17.5	57.7	31.2	2.7	303.1	87.4
RML/SiO_2(H)	16.6	3.8	1.1	35.7	18.1	59.8	32.1	3.2	327.8	101.1

[a] Reaction conditions: $T = 300$ °C, $P = 3$ MPa, catalyst: 0.3 g, and flow rate = 50 ml min^{-1} (H_2/CO = 2). Experimental error: ±5%. [b] Based on carbon efficiency, carbon selectivity = $n_iC_i/\sum n_iC_i$. [c] C_2 Oxy denotes oxygenates containing two carbon atoms. [d] HC denotes all hydrocarbons. [e] Other Oxy denotes oxygenates containing more than two carbon atoms.

similar activity in the initial stage of reaction, but showed different trends as the function of time. As shown in Fig. 1a, the CO conversion of RML/SiO_2(L) increased slowly after a slight decline at the initial stage of reaction. But the selectivity of C_2 oxygenates decreased gradually followed by the increase in hydrocarbons selectivity with the time, and the selectivity of C_2 oxygenates eventually stabilized at *ca.* 10% when the reaction time exceeded to 15 h. Because of the decrease of C_2 oxygenates selectivity, the space time yield (STY) of C_2 oxygenates decreased from the original 303.1 g (kg^{-1} h^{-1}) to 87.4 g (kg^{-1} h^{-1}) after reaction for 15 h. On the other hand, the catalytic activities of the RML/SiO_2(H) catalyst were performed quite stably as the function of time. The CO conversion kept at ~16%, and the selectivity towards to C_2 oxygenates also stabilized at ~56% in the whole reaction process. Correspondingly, the STY of C_2 oxygenates was maintained at *ca.* 300 g (kg^{-1} h^{-1}).

The reaction results showed that the catalytic performance was relatively stable on SiO_2(H) supported catalyst, however, the reactivity of the RML/SiO_2(L) catalyst changed obviously as the function of time. It is suggested that the changing of ammonia concentration played an important role in the modification of the properties of SiO_2. Correspondingly, the structure and state of the supported metals could be different on the two supports, resulting in the different catalytic performance.

3.2. Textural characterization

XRD patterns of supports and the corresponding catalysts showed no crystalline phases (Fig. 2), indicating that the SiO_2 were XRD-amorphous and the metal particles were highly dispersed on the SiO_2 support due to the small content.

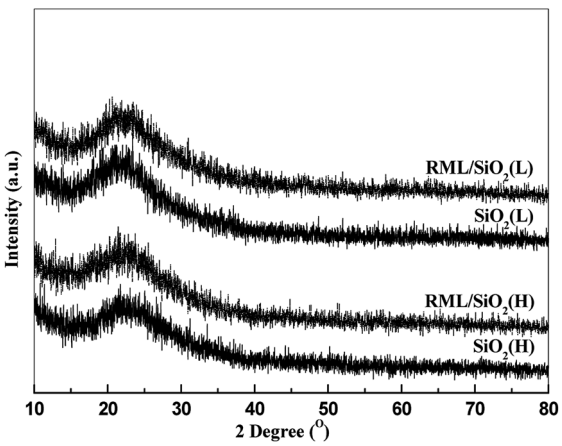

Fig. 2 The XRD patterns of supports and the corresponding catalysts.

N_2 adsorption–desorption was carried out to characterize the textural properties of the samples. It can be seen from Table 2 that the supports of SiO_2(H) and SiO_2(L) kept a similar specific surface area, average pore diameter, and pore volume. Upon being loaded with metal components, there was a slight decrease in the surface area and pore diameter for both of the catalysts. It is supposed that the loading of metal components did not have major influence on the textural properties of the supports.

The IR spectra of SiO_2 and the corresponding catalysts in N_2 atmosphere at 300 °C are presented in Fig. 3. According to the previous studies,[23,24] the region in the range 3500–2750 cm^{-1} with a maximum at 3400 cm^{-1}, originates from the absorption of H_2O and –OH interacted with hydrogen bond; and the band at 950 cm^{-1}, arises from the absorption of Si–OH. As shown in Fig. 3, it is obvious that there were more hydroxyl groups on the surface of SiO_2(L) than that of SiO_2(H), suggesting that the surface Si–OH groups on SiO_2(H) condensed more significantly. Moreover, it can be found that the IR profiles of catalysts did not change obviously compared with the corresponding supports, but the intensity of the hydroxyl groups on SiO_2 decreased after supporting metal components, suggesting that the metal components were fixed by the hydroxyl–metal interaction.

3.3. TEM

Fig. 4 shows the TEM micrographs and the corresponding Rh particle size distributions of catalysts supported on the different SiO_2. Firstly, as shown in the enlarged photographs in Fig. 4a and b, both of the particles of SiO_2(H) and SiO_2(L) were monodispersed spherical with a mean size of ~500 nm. However, compared with the SiO_2(H), the spherical surface of SiO_2(L) was more rough, meanwhile many small particles around the spheres were observed for the SiO_2(L). It is obvious that the

Table 2 Specific surface areas (S_{BET}), pore volume (V_p) and pore diameter (D_p) of supports and the corresponding catalysts

Sample	S_{BET} (m^2 g^{-1})	V_p (cm^3 g^{-1})	D_p (nm)
SiO_2(H)	11.6	0.021	7.9
RML/SiO_2(H)	10.4	0.021	6.7
SiO_2(L)	20.8	0.036	7.1
RML/SiO_2(L)	19.3	0.031	6.3

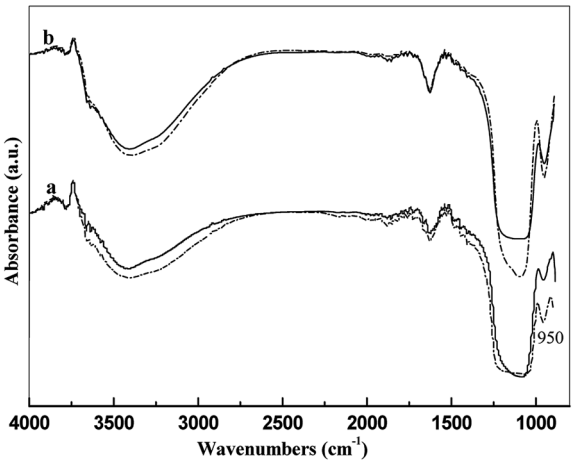

Fig. 3 The IR spectra of supports and the corresponding catalysts: (a) SiO_2(H) (the dashed line) and RML/SiO_2(H) (the straight line); (b) SiO_2(L) (the dashed line) and RML/SiO_2(L) (the straight line).

concentration of ammonia influenced the morphology of SiO_2. The high concentration of ammonia restrained the hydrolysis proceeding, thus the continuous condensation of nuclei supplied the formation of uniform spheres. In the contrast, the low concentration of ammonia speeded the hydrolysis rate, which provided more substrate reservoir for condensation, resulting in the formation of small particles and spheres with rough surface.

It can be seen that the Rh nanoparticles were highly dispersed on the fresh catalysts, and the particle size fell sharp in the range of 1–4 nm. The mean sizes of Rh particles over RML/SiO_2(H) and RML/SiO_2(L) were very close, which were 2.6 and 3.1 nm, respectively. Compared with the fresh catalysts, the mean size of Rh particles in the RML/SiO_2(H)-UD catalyst became slightly larger (3.5 nm), whereas the mean size of Rh particles in the RML/SiO_2(L)-UD increased strikingly to 8.1 nm. It is inferred that, compared with the smooth convex surface of SiO_2(H), the rough surface of SiO_2(L) looked like a huge amounts of hollows in the surface, which should be more conducive to the agglomeration of metal particles in these hollows.

Combined with the catalytic results, it is obvious that the size of Rh particles has a remarkable influence on the activity and selectivity of Rh–Mn–Li/SiO_2 for CO hydrogenation. It is conceivable that, because of the similar Rh particle size of the fresh catalysts, the initial catalytic performance over the two catalysts were almost the same. Furthermore, the catalytic activities of the RML/SiO_2(H) catalyst were found to be quite stable with the time, which should be attributed to the stable Rh particle size on the SiO_2(H) support. In contrast, the mean size of Rh particles supported on SiO_2(L) increased remarkably during the reaction process, which, in turn, was reflected by the gradual decrease of C_2 oxygenates selectivity along with the increase in hydrocarbons selectivity. As reported in the literature,[25–27] the optimal Rh particle size for the formation of C_2 oxygenates is 2–6 nm. Meanwhile, Ojeda *et al.*[28] found that as Rh particle size increased, the higher hydrocarbons formation was favored at expenses of the oxygenated compounds. These

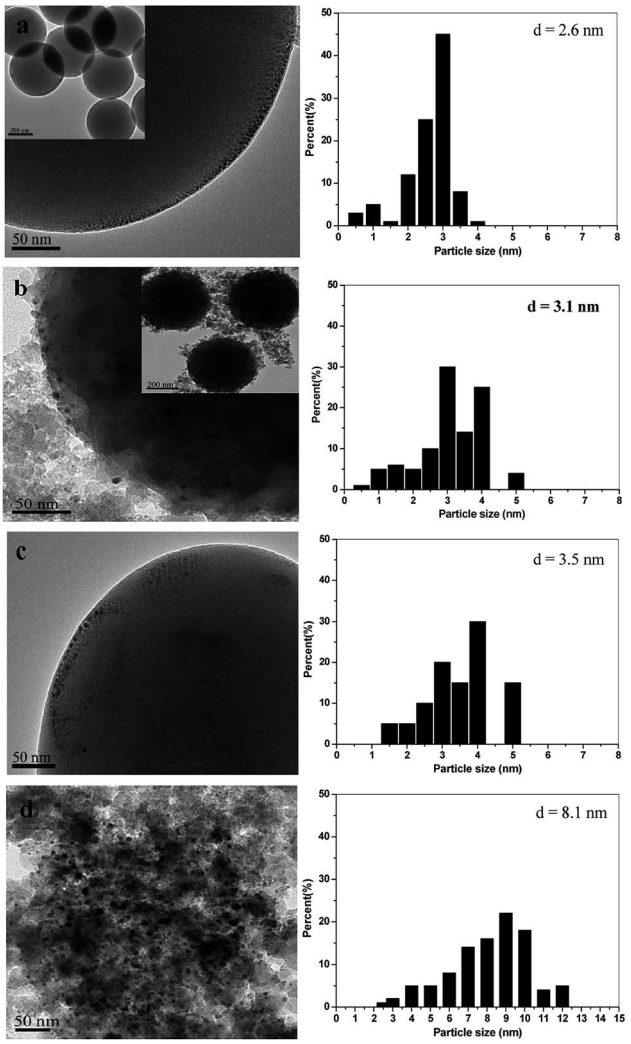

Fig. 4 TEM images and Rh particle size distributions of different catalysts: (a) RML/SiO_2(H), (b) RML/SiO_2(L), (c) RML/SiO_2(H)-UD, (d) RML/SiO_2(L)-UD.

conclusions are consistent with our results. Moreover, it is noteworthy that although the selectivities of RML/SiO_2(L) changed dramatically as the function of time, but the conversion rate was relatively stable, indicating that CO conversion is little influenced by the Rh particle size, consistent with the suggestion reported by Underwood *et al.*[29] that for Rh/SiO_2, the dispersion of Rh had little effect on the total catalyst activity, but did strongly influence product selectivity.

3.4. H_2-TPR

Fig. 5 shows the H_2-TPR profiles for both of the fresh and used catalysts. It can be seen that there were three peaks of H_2 consumption in the TPR profile of the RML/SiO_2(H) catalyst. As reported in previous paper,[30,31] the high temperature peak centered around 320 °C was ascribed to the reduction of MnO_2, and the major peak at 140 °C and the shoulder peak at 160 °C were assigned to the reduction of Rh_2O_3 not intimately contacting with Mn species (denoted as Rh(I)) and of Rh_2O_3

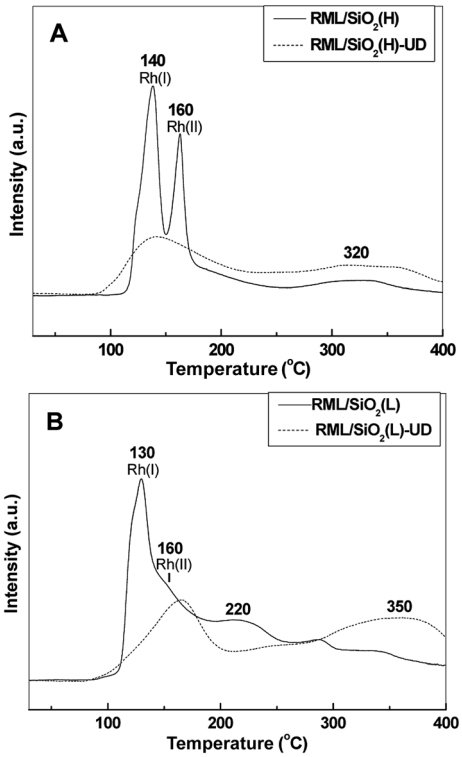

Fig. 5 H_2-TPR profiles of the catalysts: (A) RML/SiO_2(H) and RML/SiO_2(H)-UD, (B) RML/SiO_2(L) and RML/SiO_2(L)-UD.

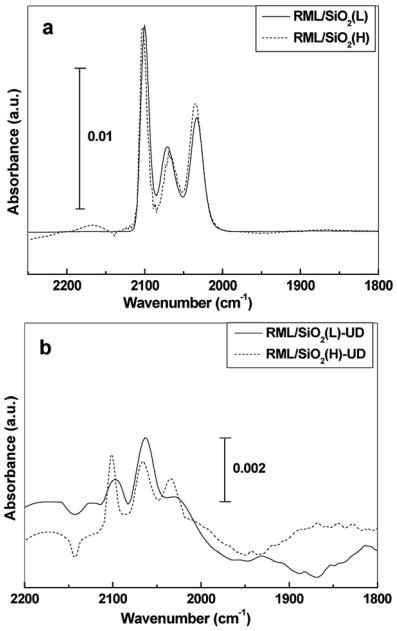

Fig. 6 FT-IR spectra of CO chemisorbed at 30 °C: (a) fresh catalysts; (b) used catalysts.

intimately contacting with Mn species (denoted as Rh(II)), respectively. Compared with the catalyst of RML/SiO_2(H), the reduction peak of Rh(I) over RML/SiO_2(L) catalyst shifted to the lower temperature (130 °C). While the peak of Rh(II) became wide along with a severe shift of the reduction peak of MnO_2 to the lower temperature (220 °C). It is inferred that the rough surface of SiO_2(L) is more conducive to the Rh–Mn interaction. From the patterns of used catalysts, it can be found that the reduction of Rh_2O_3 returned to a single wide peak, and the reduction peak area decreased obviously than that of fresh catalysts. Simultaneously, the reduction of Rh and Mn became more isolated. We inferred that, after reaction, the part of Rh and Mn clusters became to aggregate by themselves, resulting in the weakening of Rh–Mn interaction. On the other hand, the reduction temperature of Rh_2O_3 over RML/SiO_2(L)-UD catalyst was much higher than that of RML/SiO_2(H)-UD. It is further proposed that, during the reaction, the Rh and Mn particles are much easier to agglomerate on the surface of SiO_2(L) compared to that of SiO_2(H), which is consistent with the result of TEM.

3.5. FT-IR

The IR spectra of the *in situ* reduced catalysts interacting with 80 mbar CO in vacuum at 30 °C for 30 min are shown in Fig. 6. The IR spectrum was mainly composed by a band at around 2067 cm^{-1} and a doublet at ~2100 and ~2030 cm^{-1}. The 2067 cm^{-1} band can be attributed to the linear adsorbed CO [CO(l)] and the doublet can be assigned to the symmetric and asymmetric carbonyl stretching of the *gem*-dicarbonyl $Rh^+(CO)_2$[CO(gdc)].[32]

It is widely accepted that the dicarbonyl species can only be formed on the Rh^+ sites which may be highly dispersed and linear CO be on the Rh^0 sites.[33,34] As shown in Fig. 6a, both the peak intensity of adsorbed CO and the peak area ratio of CO(gdc)/CO(l) (Rh^+/Rh^0) were almost the same on the two fresh catalysts, implying that the state of Rh on both of them was quite similar. Correspondingly, at the beginning of reaction, the two catalysts showed similar catalytic properties.

The spectra of the adsorbed CO on the used catalysts in Fig. 6b showed that the intensity of adsorbed CO decreased severely compared with the fresh catalysts, suggesting that the active sites of Rh lost part of activity or were covered partly. Meanwhile, the peak area ratio of CO(gdc)/CO(l) also decreased after reaction. In more detail, the peak area ratio of CO(gdc)/CO(l) on RML/SiO_2(L)-UD become much smaller than that of RML/SiO_2(H)-UD. Considering that the CO(gdc) species can only be formed on the highly dispersed Rh^+ sites, it is concluded that the Rh supported on SiO_2(L) is easier to aggregation compared with those supported on SiO_2(H), which is also consistent with the result of TEM.

Combined with the reaction data, it is inferred that the relatively stable ratio of Rh^+/Rh^0 is correlated to the steady catalytic performance of RML/SiO_2(H) in the reaction process. Ichikawa and co-workers[35] proposed that Rh^0 is active for CO dissociation and Rh^+ is active for CO insertion, and, correspondingly, the changing of ratio of Rh^+/Rh^0 will change the catalytic properties. Chuang and Pien also suggested that the presence of isolated Rh^+ sites may contribute to the increased selectivity for higher oxygenates.[36] According to the above propositions, we inferred that, because the ratio of Rh^+/Rh^0 on RML/SiO_2(L) would decrease markedly during the reaction, the hydrocarbons formation was favored at expenses of oxygenated compounds as the function of time.

3.6. TPSR

Fig. 7 displays the TPSR profiles of the samples. It can be seen that there was one main methane peak at 240 °C in the profiles of the fresh catalysts, both the location and peak area for the two catalyst were almost the same. It is indicated that the number and property of active sites responsible for methane production are equivalent on the fresh catalysts, which can also be reflected by the similar selectivity of hydrocarbons at the beginning of reaction. In addition, the broad peak centered at 520 °C in the pattern of RML/SiO_2(H) might be due to the hydrogenation of carbon species formed at lower temperatures and transformed to a less active form.[37]

The TPSR experiments over the used catalysts are also showed in Fig. 7 in order to compare with the fresh samples. Compared with the catalyst of RML/SiO_2(H), one peak of CH_4 formation at about 240 °C also appeared on RML/SiO_2(H)-UD, however, the peak area decreased strikingly. It is inferred that the state of Rh may not change evidently, but the number of Rh sites on RML/SiO_2(H) decreased after reaction caused by the coverage of the high boiling products, which is in line with the result of IR. On the profile of RML/SiO_2(L)-UD, the CH_4 peak was centered at around 275 °C, which shifted to the higher temperature compared to that of RML/SiO_2(L). The shifting of the CH_4 peak should be attributed to the aggregation of Rh particles supported on SiO_2(L), which is good agreement with the results of TEM and TPR. By combining the catalytic properties of the catalysts and above discussions, it can be suggested that the stable catalytic properties of RML/SiO_2(H) is attributed to the steady state of Rh; on the contrary, the aggregation of Rh particles supported on SiO_2(L) is viewed as an important factor affecting selectivity.

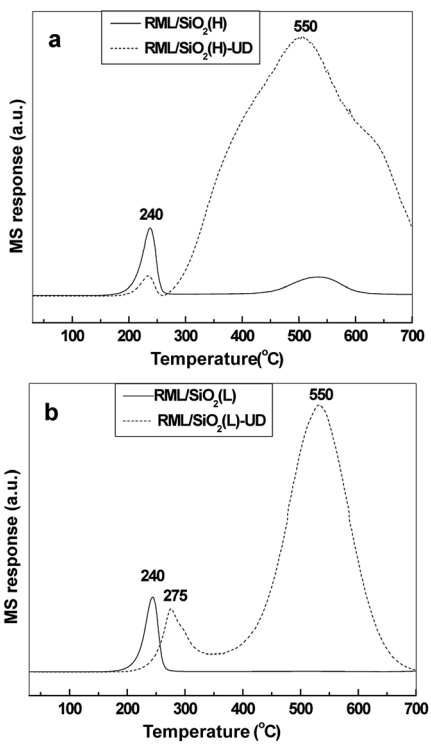

Fig. 7 TPSR profiles of the catalysts for CH_4 formation: (a) RML/SiO_2(H) and RML/SiO_2(H)-UD, (b) RML/SiO_2(L) and RML/SiO_2(L)-UD.

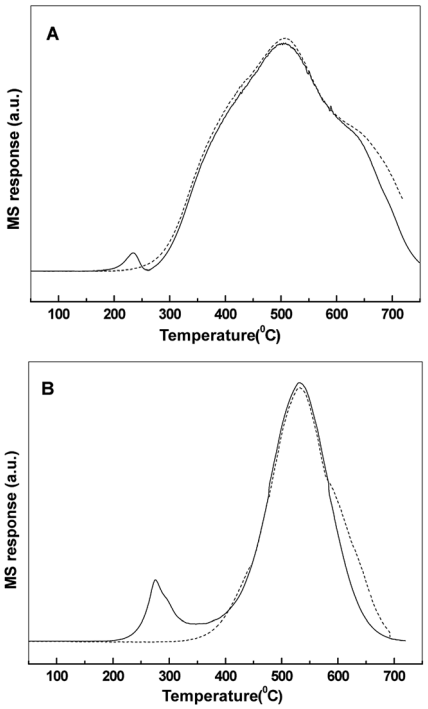

Fig. 8 The TPSR profiles (the straight lines) and temperature procedure experiment profiles in the flow of H_2 without CO pro-absorption (the dash lines): (A) RML/SiO_2(H)-UD; (B) RML/SiO_2(L)-UD.

In addition, a wide peak of CH_4 at the range of 300–700 °C appeared on both of the used catalysts. Since the peak area was too large, it should not be formed by the hydrogenation of adsorbed CO. In order to confirm where it came from, the temperature procedure experiment over the used catalysts in the flow of H_2 without CO pro-absorption was used to compare with the TPSR profiles, as shown in Fig. 8. It can be seen that the profiles obtained without CO pro-absorption just appeared one peak at the range of 300–700 °C, which coincided with the second peak of TPSR profiles of the used catalysts. This observation clearly indicated that the peak at the range of 300–700 °C should be formed by the hydrogenation of carbon disposition on the used catalysts.

4. Conclusions

Two Rh–Mn–Li catalysts supported on the monodispersed SiO_2 synthesized by the Stöber method with different ammonia concentration were tested for the synthesis of C_2 oxygenates *via* CO hydrogenation. The reaction results showed that the catalytic performance was relatively stable on SiO_2(H) supported catalyst, however, the reactivity of the RML/SiO_2(L) catalyst changed obviously as the function of time.

The results proved that the changing of ammonia concentration played an important role in the modification of the properties of SiO_2. Correspondingly, the structure and state of the supported metals could be different on the two supports.

The stable catalytic properties of RML/SiO_2(H) is attributed to the relatively steady state of Rh in the reaction process. On the contrary, the rough surface of SiO_2(L) resulted in easy agglomeration of the metals and decrease of the isolated Rh^+ sites, thus the higher hydrocarbons formation was favored at expenses of the oxygenated compounds over the RML/SiO_2(H) catalyst as the function of time.

Acknowledgements

The authors gratefully acknowledge financial support from the Science and Technology Commission of Shanghai Municipality (08520513600), Leading Academic Discipline Project of Shanghai Education Committee (J51503) and Shanghai Municipal Science and Technology Commission (13ZR1461900).

Notes and references

1 J. R. Rostrup-Nielsen, *Science*, 2005, **308**, 1421.
2 V. Subramani and S. K. Gangwal, *Energy Fuels*, 2008, **22**, 814.
3 J. J. Spivey and A. Egbebi, *Chem. Soc. Rev.*, 2007, **36**, 1514.
4 D. H. Mei, R. Rousseau, S. M. Kathmann, V. A. Glezakou, M. H. Engelhard and W. L. Jiang, *J. Catal.*, 2010, **271**, 325.
5 G. C. Chen, C. Y. Guo, X. H. Zhang, Z. J. Huang and G. Q. Yuan, *Fuel Process. Technol.*, 2011, **92**, 456.
6 M. A. Haider, M. R. Gogate and R. J. Davis, *J. Catal.*, 2009, **261**, 9.
7 S. S. C. Chuang, R. W. Stevens Jr and R. Khatri, *Top. Catal.*, 2005, **32**, 225.
8 J. P. Hindermann, G. J. Hutchings and A. Kiennemann, *Catal. Rev.: Sci. Eng.*, 1993, **35**, 1.
9 S. Ho and Y. Su, *J. Catal.*, 1997, **168**, 51.
10 D. H. Jiang, Y. J. Ding, Z. D. Pan, W. M. Chen and H. Y. Luo, *Catal. Lett.*, 2008, **121**, 241.
11 F. Solymosi, I. Tombacz and M. Kocsis, *J. Catal.*, 1982, **75**, 78.
12 P. Basu, D. Panayotov and J. T. Yates Jr, *J. Am. Chem. Soc.*, 1988, **110**, 2074.
13 E. Guglielminotti, F. Pinna, M. Rigoni, G. Strukul and L. Zanderighi, *J. Mol. Catal. A: Chem.*, 1995, **103**, 105.
14 H. M. Yin, Y. J. Ding, H. Y. Luo, H. J. Zhu, D. P. He, J. M. Xiong and L. W. Lin, *Appl. Catal., A*, 2003, **243**, 155.
15 H. Y. Luo, P. Z. Lin, S. B. Xie, H. W. Zhou, C. H. Xu, S. Y. Huang, L. W. Lin, D. B. Liang, P. L. Yin and Q. Xin, *J. Mol. Catal. A: Chem.*, 1997, **122**, 115.
16 H. Arakawa, T. Fukushima, M. Ichikawa, S. Natsushita, K. Takeuchi, T. Matsuzaki and Y. Sugi, *Chem. Lett.*, 1985, **14**, 881.
17 X. Mo, J. Gao, N. Umnajkaseam and J. G. Goodwin Jr, *J. Catal.*, 2009, **267**, 167.
18 J. Yu, D. S. Mao, L. P. Han, Q. S. Guo and G. Z. Lu, *Catal. Commun.*, 2012, **24**, 25.
19 J. Yu, D. S. Mao, L. P. Han, Q. S. Guo and G. Z. Lu, *J. Mol. Catal. A: Chem.*, 2013, **367**, 38.
20 W. M. Chen, Y. J. Ding, D. H. Jiang, Z. D. Pan and H. Y. Luo, *Catal. Lett.*, 2005, **104**, 177.
21 X. L. Pan, Z. L. Fan, W. Chen, Y. J. Ding, H. Y. Luo and X. H. Bao, *Nat. Mater.*, 2007, **6**, 507.
22 M. Szekeres, O. Kamalin, P. G. Grobet, R. A. Schoonheydt, K. Wostyn, K. Clays, A. Persoons and I. Dkénáy, *Colloids Surf., A*, 2003, **227**, 77.
23 P. Basu, D. Panayotov and J. T. Yates Jr, *J. Am. Chem. Soc.*, 1988, **110**, 2074.
24 J. B. Peri, *J. Phys. Chem.*, 1966, **70**, 2937.
25 Z. L. Fan, W. Chen, X. L. Pan and X. H. Bao, *Catal. Today*, 2009, **147**, 86.
26 H. Hamada, R. Funaki, Y. Kuwahara, K. Wakabayashi and T. Ito, *Appl. Catal.*, 1987, **30**, 177.
27 T. Hanaoka, H. Arakawa, T. Matsuzaki, Y. Sugi, K. Kanno and Y. Abe, *Catal. Today*, 2000, **58**, 271.
28 M. Ojeda, S. Rojas, M. Boutonnet, F. J. Pérez-Alonso, F. J. García-García and J. L. G. Fierro, *Appl. Catal., A*, 2004, **274**, 33.
29 R. P. Underwood and A. T. Bell, *Appl. Catal.*, 1987, **34**, 289.
30 J. Yu, D. S. Mao, L. P. Han, Q. S. Guo and G. Z. Lu, *Fuel Process. Technol.*, 2013, **106**, 344.
31 D. H. Jiang, Y. J. Ding, Z. D. Pan, X. M. Li, G. P. Jiao, J. W. Li, W. M. Chen and H. Y. Luo, *Appl. Catal., A*, 2007, **331**, 70.
32 S. D. Worley, G. A. Mattson and R. Caudlll, *J. Phys. Chem.*, 1983, **87**, 1671.
33 R. R. Cavanagh and J. T. Yates Jr, *J. Chem. Phys.*, 1981, **74**, 4150.
34 C. A. Rice, S. D. Worley, C. W. Curtis, J. A. Guin and A. R. Tarrer, *J. Chem. Phys.*, 1981, **74**, 6487.
35 M. Kawai, M. Uda and M. Ichikawa, *J. Phys. Chem.*, 1985, **89**, 1654.
36 S. S. C. Chuang and S. I. Pien, *J. Catal.*, 1992, **138**, 536.
37 Y. Wang, H. Y. Luo, D. B. Liang and X. H. Bao, *J. Catal.*, 2000, **196**, 46.

